11th Asia-Pacific Conference on Combustion,
The University of Sydney, NSW Australia
10th-14th December 2017.

Reduction Methodology for Detailed Kinetic Mechanisms: Application to *n*-Hexane-Air Hot Surface Ignition

S. Coronel[1,*], J. Melguizo-Gavilanes[1], D. Davidenko[2], R. Mével[3,4], J. E. Shepherd[1]
[1]California Institute of Technology, Pasadena, USA
1200 E. California Blvd, MC 205-45, Pasadena, California 91125, USA
[2]The French Aerospace Lab ONERA, Palaiseau, France
[3]Center for Combustion Energy, [4]Department of Automotive Engineering, Tsinghua University
30 Shuang Qing road, 100084 Beijing, China

Abstract

A reduction method for detailed kinetic mechanisms is presented. The reduction procedure was performed by using the ignition delay time as the target parameter. Overall, good qualitative and quantitative comparison was observed between the reduced mechanism results and experimental parameters such as ignition delay time, laminar burning speed, and concentrations in a jet-stirred reactor. The resulting reduced mechanism was used in multi-dimensional numerical simulations to predict the ignition behavior and thresholds of reactive gas adjacent to hot surfaces. Errors of less than 10% were observed between the numerical and experimental ignition thresholds indicating the adequacy of the reduction procedure.

1 Introduction

Accidental hot surface ignition is a problem of interest in the manufacturing, nuclear and mining sectors, and in aviation [1]. Significant progress has been made to experimentally understand hot surface ignition, in particular as it is applied to aviation safety [2, 3]. Typically, *n*-hexane has been used as a single component surrogate of kerosene since it exhibits a relatively high vapor pressure which facilitates testing at ambient conditions. Collecting test data is time consuming and costly since a large number of hot surface geometries and mixture conditions mus be tested. While performing multi-dimensional numerical simulations is an appealing alternative to experiments; predictive simulations require the use of detailed chemical mechanisms to predict the ignition and flame propagation events. Detailed reaction models for hydrocarbon fuels typically consist of hundreds of species and thousands of reactions. It is not feasible with existing computational resources to use these mechanisms in direct numerical simulations to model engineering tests or applications. An alternative is to use a reduced chemical mechanism that will still predict the appropriate target parameters such as ignition delay time of a full detailed mechanism. The current study describes the reduction for a *n*-hexane chemical mechanism. Comparisons are made between, 0D and 1D models that use the reduced mechanism and experimental results, and finally the resulting mechanism is applied to several multi-dimensional numerical simulations of thermal ignition.

*Corresponding author: coronel@caltech.edu

2 Materials and Methods

A modified version of the reduction procedure presented in [4] was employed. The reduction is controlled by the accuracy of one target phenomenon, the auto-ignition process. More specifically, the target parameters are: time to peak thermicity, maximum thermicity, equilibrium temperature, equilibrium mean molar mass, and temporal profiles of, thermicity, temperature, and mean molar mass. The reduction is performed as follows:

1. Calculate the error in the target parameters introduced by deactivating one species and all associated reactions; the error score at each deactivation step is given by
$$s_q = \epsilon_q / \epsilon_q^*, \tag{1}$$
where,
$$\epsilon_q = |q - q^{\text{ref}}| / q^{\text{ref}}. \tag{2}$$
q^{ref} is the target parameter calculated by using the complete detailed mechanism, q is the target parameter with the reduced mechanism, and ϵ_q^* is a user defined error limit. The error score is calculated across various conditions of initial temperature, T_0, initial pressure, P_0, and equivalence ratio, Φ. The sum S corresponds to the $\sum s_q$ across all the conditions tested.

2. Reactive species and all associated reactions and return to step 1 to deactivate the next species, repeat until S has been computed for each deactivated species.

3. Eliminate a single species with the lowest S value and all associated reactions and return to step 1. This sequence is applied until S reaches a user defined value of S^*.

The procedure described above was applied to the detailed chemical mechanism of Mével [5] which consists of 531 species and 2628 reactions. The mechanism was reduced for the following range of conditions: $T_0 = 800 - 1600$ K, $P_0 = 1$ atm, and $\Phi = 0.9$. The final reduced mechanism consists of 62 species and 223 reactions.

3 Results and Discussion

Several experimental parameters were compared against calculations performed in Cantera [6] using the reduced mechanism. Shock tube ignition delay time data were compared against numerical values obtained in a constant volume adiabatic reactor, experimental flame speeds were compared against 1D freely propagating flame calculations and jet-stirred reactor (JSR) experimental mole fractions were compared against perfectly-stirred reactor (PSR) model calculations.

3.1 Ignition Delay Time

n-Hexane shock tube ignition delay time data were taken from [7, 8]. Figure 1 shows comparisons between the model and experimental results at $\Phi = 0.5$ and 1.0. The experimental values lie significantly above the model results at $\Phi = 2.0$. Overall, at $P = 350$ kPa, the root-mean-square error (RMSE), is 29 μs, 131 μs, and 132 μs at $\Phi = 0.5$, 1.0, and 2.0, respectively.

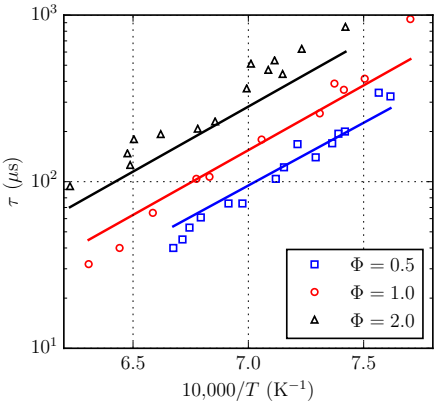

Figure 1: Experimental [7] (symbols) and model (solid lines) ignition delay time of *n*-hexane-O_2-Ar at $P = 350$ kPa. Argon mass fraction is 0.96.

Figure 2 shows experimental and simulated ignition delay time results at $P = 1.27$ and 6.13 MPa at $\Phi = 0.5$. The experimental values lie very close to the model results at $P = 1.27$ MPa. At $P = 6.13$ MPa, the model reproduces the ignition delay times at high temperatures and deviates slightly from the experimental values at lower temperatures. At $P = 1.27$ and 6.13 MPa, the RMSE is equal to 47 μs and 107 μs, respectively.

3.2 Laminar Burning Speed

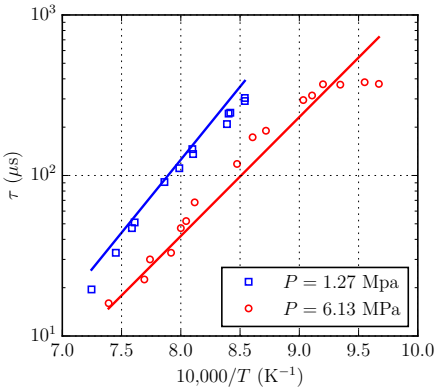

Figure 2: Experimental [8] (symbols) and model (solid lines) ignition delay time of *n*-hexane-air at $\Phi = 0.5$.

After the chemical mechanism was reduced with the ignition delay time as the target parameter, the reduced mechanism was applied to 1D freely propagating flame simulations and the results are compared against *n*-hexane-air experimental laminar burning speeds obtained from [9, 10]. Figure 3 shows that the model over-estimates the experimental values for lean conditions and lies within the uncertainty of the experimental values for rich conditions. The RMSE is 3.6 cm/s and 2.5 cm/s when comparing the model against the results from [9] and [10], respectively. Although the mechanism was reduced by using the auto-ignition process as the target phenomenon, reasonable agreement is observed between the experimental laminar burning speeds and the 1D freely propagating flame simulations. This suggests that if the laminar burning speed is chosen as the target phenomenon, then reasonable agreements between the model and the ignition delay time would also be obtained.

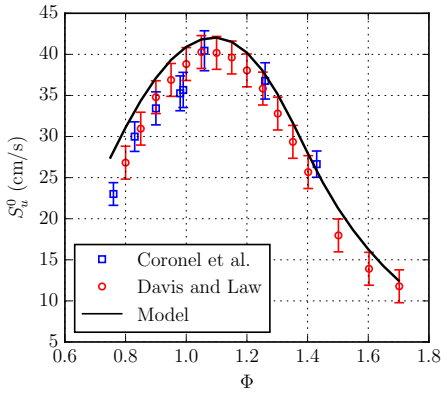

Figure 3: Experimental [9, 10] (symbols) and calculated (solid line) laminar burning speeds of *n*-hexane-air at $T = 300$ K and $P = 100$ kPa.

3.3 Jet-Stirred Reactor (JSR)

A perfectly-stirred reactor model was used with the reduced chemical mechanism to compare against jet-stirred reactor experimental results from [11]. The experimental values were obtained for the oxidation of

n-hexane at $P = 10$ atm and $\Phi = 1.0$. The normalized root-mean-square error (NRMSE) shown in Table 1 is calculated for species mole fractions shown in Figs. 4 and 5.

Species	NRMSE	Species	NRMSE
n-C_6H_{14}	0.35	H_2	0.5
O_2	0.15	CH_4	1.4
H_2O	0.48	CH_2O	0.4
CO_2	0.7	C_3H_6	1.2
CO	1.2	CH_3CHO	0.6
C_2H_4	10.6	C_4H_8-1	0.4

Table 1: NRMSE between jet-stirred reactor experimental values and model results.

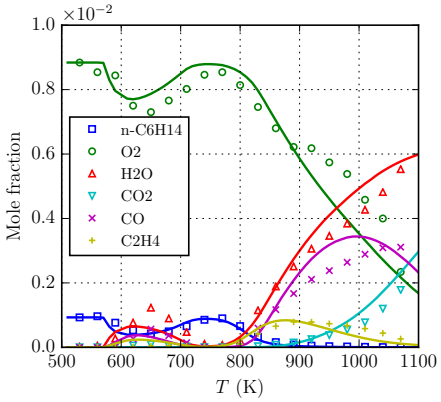

Figure 4: Experimental [11] (symbols) and modeling (solid lines) results for n-hexane oxidation in a jet-stirred reactor at $P = 10$ atm and $\Phi = 1.0$; only major species are shown.

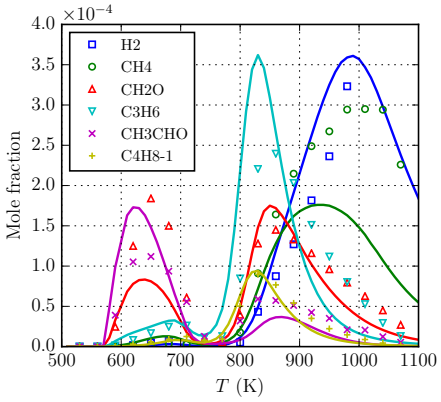

Figure 5: Experimental [11] (symbols) and modeling (solid lines) results for n-hexane oxidation in a jet-stirred reactor at $P = 10$ atm and $\Phi = 1.0$; only minor species are shown.

Based on the values of NRMSE, the model increases in accuracy for the major species in the following order: $C_2H_4 \rightarrow CO \rightarrow CO_2 \rightarrow H_2O \rightarrow n\text{-}C_6H_{14} \rightarrow O_2$. The model increases in accuracy for the minor species in the following order: $CH_4 \rightarrow C_3H_6 \rightarrow CH_3CHO \rightarrow H_2 \rightarrow CH_2O \rightarrow C_4H_8$-1

3.4 Multi-Dimensional Numerical Calculations

Finally, the reduced mechanism was applied to two-dimensional numerical simulations of thermal ignition using the OpenFOAM framework [12]. The motion, transport and chemical reaction in the gas were modeled using the variable-density, reactive Navier-Stokes equations with temperature-dependent transport properties. Differential diffusion was included using a constant non-unity Lewis number for each species. A detailed description of the model can be found in [13]. The problem simulated is ignition of n-hexane-air at $\Phi = 0.9$, $T_0 = 300$ K, and $P_0 = 100$ kPa, by heated surfaces of $6 - 10$ mm in size. Several configurations, shown in Fig. 6, were tested. Filled contours of CO_2 mass fraction are shown in Fig. 6; the images correspond to ignition events taking place when the surface temperature is at the ignition threshold.

A commercially available glow plug (9.3 mm in height and 5.1 mm in diameter) was simulated in Fig. 6 (a). A temperature ramp of 220 K/s was imposed at the surface; the heat from the surface diffuses into the gas and is convected upwards forming a hot plume. Ignition occurred in a stagnation point located above the top surface of the glow plug. The concentration of CO_2 was used to pinpoint and visualize the ignition location. A moving hot sphere (6 mm in diameter) was simulated in Fig. 6 (b). The sphere had a surface temperature of 1300 K and was moving at 2.4 m/s. A thermal boundary layer developed around the moving hot sphere. At the temperature and velocity given, the flow is laminar and axisymmetric with a toroidal vortex in the wake. The flow also has a separation region (marked by the high concentration of CO_2) due to adverse pressure gradients. It is in this region of flow separation were ignition takes place. A vertical cylinder with a heated area of 10 mm in height was simulated in Fig. 6 (c). A temperature ramp of 220 K/s was imposed at the surface. Thermal and hydrodynamic boundary layers grow upwards along the cylinder surface. Ignition takes place in the gas at a height corresponding with the top boundary of the heated surface. Finally, a horizontal cylinder (10 mm in diameter) was simulated in Fig. 6 (d). A temperature ramp of 220 K/s was imposed at the surface. There is growth of the thermal and momentum boundary layers from the front stagnation point to the rear stagnation point. Ignition takes place in the rear stagnation point where the temperature gradients are smallest.

Geometry	Exp. (K)	Calc. (K)	$\Delta T/T_{\text{exp}}$
Hor. Cyl. [14]	1180	1093	0.07
Vert. Cyl. [14]	1270	1191	0.06
Sphere [3]	1224	1300	0.06
Glow Plug [15]	1275	1162	0.09

Table 2: Comparison of experimental and numerical results for all hot surface geometries tested.

Experimental and predicted ignition thresholds for all the geometries considered are shown in Table 2. Normalized differences, $\Delta T/T_{\text{exp}}$, were calculated between

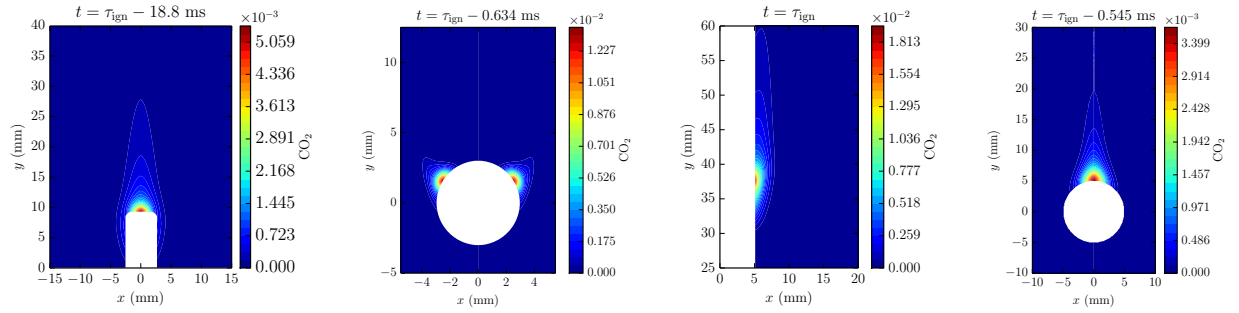

(a) Glow plug (b) Moving sphere (c) Vertical cylinder (d) Horizontal cylinder

Figure 6: CO_2 mass fraction fields at the ignition event using a (a) glow plug, (b) moving sphere, (c) vertical cylinder, and (d) horizontal cylinder.

the ignition thresholds obtained numerically, T_{calc}, and experimentally, T_{exp}; ΔT is equal to $|T_{exp} - T_{calc}|$. Regardless of the geometric configuration of the hot surface, the difference between the numerical and experimental results was less than 10%. The multi-dimensional simulations indicate that ignition can be predicted using the reduced n-hexane mechanism presented in this study.

4 Conclusions

A reduction methodology for detailed kinetic mechanisms was described and applied to obtain a reduced mechanism for n-hexane. The reduced mechanism predictions using a constant volume adiabatic reactor showed good quantitative comparison with experimental ignition delay time measurements. Although not reduced for flame speed calculations, the reduced mechanism performs well when applied to a 1D freely propagating flames. Jet-stirred reactor results indicated good quantitative comparison for the major and minor species presented. Finally, the reduced mechanism was applied to a two-dimensional simulation of ignition by heated surfaces and resulted in differences of less than 10% when compared against experimental ignition measurements.

5 Acknowledgements

This work was carried out in the Explosion Dynamics Laboratory of the California Institute of Technology, and was supported by The Boeing Company through a Strategic Research and Development Relationship Agreement CT-BA-GTA-1.

References

[1] Stack B., Sepeda A. and Moosemiller M., Process Safety Progress, 33 (2014) 19–25.

[2] Boettcher P.A., Ph.D. thesis, California Institute of Technology (2012).

[3] Coronel S., Ph.D. thesis, California Institute of Technology (2016).

[4] Davidenko D., Mével R. and Dupré G., in Proceedings of the European Combustion Meeting 2009.

[5] Mével R., Chatelain K., Boettcher P.A. and Shepherd J.E., Fuel, 126 (2014) 282–293.

[6] Goodwin D.G., Moffat H.K. and Speth R.L., Cantera: An object-oriented software toolkit for chemical kinetics, thermodynamics, and transport processes, http://www.cantera.org (2017), version 2.3.0.

[7] Mével R., Niedzielska U., Melguizo-Gavilanes J., Coronel S. and Shepherd J.E., Combustion Science and Technology, 188 (2016) 2267–2283.

[8] Zhukov V.P., Sechenov V.A. and Starikovskii A.Y., Combustion and Flame, 136 (2004) 257–259.

[9] Coronel S., Lapointe S., Mével R. and Shepherd J., in Preparation for Fuel.

[10] Davis S.G. and Law C., Combustion Science and Technology, 140 (1998) 427–449.

[11] Zhang K., Banyon C., Togbé C., Dagaut P., Bugler J. and Curran H.J., Combustion and Flame, 162 (2015) 4194 – 4207.

[12] Weller H.G., Tabor G., Jasak H. and Fureby C., Comput. Phys., 12 (1998) 620–631.

[13] Melguizo-Gavilanes J., Coronel S., Mével R. and Shepherd J., International Journal of Hydrogen Energy, 42 (2017) 7380–7392.

[14] Boeck L., Meijers M., Kink A., Mével R. and Shepherd J.E., Combustion and Flame, (2017), in press.

[15] Melguizo-Gavilanes J., Nové-Josserand A., Coronel S., Mével R. and Shepherd J.E., Combustion Science and Technology, 188 (2016) 2060–2076.